Journal of Chromatography A, 1219 (2012) 1–14

Contents lists available at SciVerse ScienceDirect

Journal of Chromatography A

journal homepage: www.elsevier.com/locate/chroma

Review

Monolithic bed structure for capillary liquid chromatography

Pankaj Aggarwal[a], H. Dennis Tolley[b], Milton L. Lee[a,*]

[a] Department of Chemistry and Biochemistry, Brigham Young University, Provo, UT 84602, USA
[b] Department of Statistics, Brigham Young University, Provo, UT 84602, USA

ARTICLE INFO

Article history:
Received 27 September 2011
Accepted 25 October 2011
Available online 2 November 2011

Keywords:
Liquid chromatography
Capillary columns
Monolithic stationary phases
Morphology
Pore structure

ABSTRACT

Monolithic stationary phases show promise for LC as a result of their good permeability, ease of preparation and broad selectivity. Inorganic silica monoliths have been extensively studied and applied for separation of small molecules. The presence of a large number of through pores and small skeletal structure allows the chromatographic efficiencies of silica monoliths to be comparable to columns packed with 5 μm silica particles, at much lower back pressure. In comparison, organic polymeric monoliths have been mostly used for separation of bio-molecules; however, recently, applications are expanding to small molecules as well. Organic monoliths with high surface areas and fused morphology rather than conventional globular morphology have shown good performance for small molecule separations. Factors such as domain size, through-pore size and mesopore size of the monolithic structures have been found to govern the efficiency of monolithic columns. The structure and performance of monolithic columns are reviewed in comparison to particle packed columns. Studying and characterizing the bed structures of organic monolithic columns can provide great insights into their performance, and aid in structure-directed synthesis of new and improved monoliths.

Contents

* Corresponding author. Tel.: +1 801 422 2135; fax: +1 801 422 0159.
E-mail address: milton_lee@byu.edu (M.L. Lee).

0021-9673/$ – see front matter © 2011 Elsevier B.V. All rights reserved.
doi:10.1016/j.chroma.2011.10.083

1. Introduction

Chromatography is a separation technique based on differential distribution of solute molecules between a stationary phase and mobile phase. The properties of these two phases, more importantly the stationary phase, govern the column performance and separation efficiency. The stationary phase bed structure generally has both small mesopores as well as large through-pores, making them suitable for small as well as large molecule separations, although the separation of large molecules does not necessarily require small pores. The small mesopores give rise to large surface area required for retention of solutes and, hence, resolution. On the other hand, the distribution and size of large pores (i.e., through-pores) control column efficiency and hydraulic impedance, as they allow the mobile phase to flow through the bed. A large through-pore size and wide distribution offer high column permeability, however, at the expense of efficiency, since, a wide through-pore size distribution results in an increase in eddy diffusion contribution in the van Deemter equation. Thus, optimization of the bed structure to optimize the chromatography, i.e., good efficiency and high permeability, requires compromise, as these characteristics are inversely related. Therefore, the bed structure has been extensively investigated to achieve the best efficiency, keeping in mind the compromise between performance and practical constraints.

Stationary phases most commonly used today are particulate or monolithic in nature. Particle packed columns have long been used as stationary phases, starting from Tswett's [1] work with column beds packed with fine particles. Since then, there has been significant progress in column performance with the advent of small particles (5 μm and less) and small dimension columns, such as capillary columns and microfluidic devices [2,3]. However, these advancements have all resulted in an increase in hydraulic resistance of the column, thereby increasing the analysis time and/or necessitating the use of high pressure pumps. This tradeoff between efficient separation and analysis time was clearly demonstrated by Knox and Saleem [4], which (along with some technical problems associated with capillary column packing) has dampened some enthusiasm for these columns as particle size approaches 1 μm. There are no real possibilities of increasing the permeability of these packed beds, as any increase in permeability eventually leads to imperfections and, hence, poor performance. Therefore, there has been a need for new stationary phases capable of permitting efficient separation with good permeability.

Recent improvements in monolithic columns and core–shell particles represent major developments in the design of liquid chromatographic columns. These two stationary phase types offer the potential for satisfying the requirement of columns having good efficiency and high permeability [5]. Core–shell particles have a solid core surrounded by a porous outer layer, enabling the mobile phase to penetrate only the shell and not the core. Since larger particles are used, core–shell particles lead to reduced backpressure of the column in comparison to columns packed with porous particles. In contrast, monoliths are integrated, continuous porous separation media with no inter-particular voids and an open macropore structure. The porous layer structure and larger diameter of core–shell particles and the open macropore structure of monolithic columns permit rapid separation of analytes at reasonable back pressure, while retaining good separation efficiency.

As discussed above, the properties of these stationary phases are influenced by their bed structures, either in terms of efficiency or resistance to flow. It is the bed structures of these different types of stationary phases, particle packed (fully porous or core–shell) and monolithic (polymeric or silica), that make them so different. The cross-sectional area of a monolithic skeleton is also typically less than that of particles in packed columns. This reduced dimension of the stationary phase facilitates mass transfer from the stationary phase to the mobile phase, thereby potentially improving column efficiency. Also, the voids (through-pores) in particle packed columns result from the inter-particle space, which in turn is a function of the particle size. In organic polymer monoliths, they arise due to the presence of porogens. In silica monoliths, through-pores are formed during phase separation occurring through spinodal decomposition as a result of the porogen (such as polyethylene glycol), while smaller mesopores are formed during the aging process. The through-pores are more tortuous and constricted in packed bed structures as compared to monolithic structures, thereby adding to decreased permeability compared to monolithic beds [6]. The major advantage of monolithic bed structure over particle packed columns is that the size of the through-pores and microglobules can be tailored independently. In particle packed columns, the through-pores are simply a function of particle size and cannot be optimized independently. In comparison to monolith bed structure, the homogeneity and, hence, the performance of a particle packed bed structure is controlled by the particle size, particle size distribution and packing method.

The bed structure of these two stationary phase types is also different along the column walls, apart from that in the bulk. The particles along the walls in the particle packed column may be loosely or more tightly packed, depending on the packing procedure. On the other hand, polymeric monoliths fabricated in capillary columns are firmly attached to the capillary wall, thereby eliminating the column heterogeneity arising due to column packing. Although some radial heterogeneity occurs in monolithic columns as a consequence of different polymerization rates or porogen compositions at different locations along the column radius, it is much less than that in a particle packed column. This heterogeneity in the column greatly degrades the column performance whether it is a particle packed column or a monolithic column.

Apart from these structural differences, monoliths have many advantages in terms of production time and equipment requirements. In situ polymerization of the monolithic stationary phase is especially useful for fabrication of capillary columns in contrast to packing of particles, which requires high pressure pumps. Since monoliths are bonded to the wall, there is no need for frits at the ends of the capillary column. Moreover, their ease of surface modification along with high stability make them an attractive alternative to conventional particle packed columns for capillary column chromatography. However, monolithic columns are still in

their infancy, and require much more research to optimize their design and preparation for improved performance.

In addition to these differences between particle packed and monolithic columns, the morphologies of the monoliths vary among themselves. The skeleton of a monolith may be a globular or fused mass with no distinct microglobules, depending upon the monomer and porogen compositions. The morphology also differs between inorganic silica monoliths and organic polymeric monoliths. Inorganic silica monoliths have a significant fraction of small mesopores in the skeleton formed as a consequence of treatment with ammonia or urea as a second step in the synthesis. Organic polymeric monoliths typically lack a significant fraction of mesopores [7]. However, recently there have been a number of publications reporting use of special procedures and/or reagents during synthesis to generate mesopores in the organic polymeric skeleton such as use of surfactants as template molecules [8], early termination of the polymerization reaction [9] and hyper-crosslinking of the monolith using Friedal Crafts reaction as the second step in monolith development [10].

This review describes the bed structures of organic monoliths in comparison to structures of silica monoliths and particle beds. Factors influencing the various morphologies and their effects on chromatographic performance are also reviewed. This review has been divided into five sections. The first section discusses the techniques used for characterizing chromatographic columns. The second section describes packed column bed structure with emphasis on bed heterogeneity in the bulk and at the walls, as well as mobile phase flow through the bed. Because particle packed columns have long been studied, their bed structures can provide beneficial insights in understanding the dependence of column performance on bed structure. The third section emphasizes general monolith technology, followed by descriptions of silica and organic polymeric monolith bed structures, with greater emphasis on polymeric monoliths. These polymeric monoliths have different morphologies and pore structures, depending on the conditions of polymerization and the monomers themselves. The last section describes future efforts needed to improve efficiency and to increase the applicability of monolithic columns.

2. Techniques for characterizing chromatographic columns

Since the bed structure of the stationary phase governs the column performance, careful characterization of bed structure should aid further improvement in performance. Particle packed columns have been characterized by particle shape, size and distribution. Monolithic chromatographic columns can also be characterized by their particle/globule size and pore-size distribution, which are known to directly affect column performance. This characterization (for particulate or monolithic columns) can be done by microscopic techniques such as scanning electron microscopy (SEM) [11], X-ray analysis and transmission electron microscopy (TEM) [12]. These techniques give information about the morphology of monoliths (globular or fused) and their homogeneity along the radial direction. They provide actual images of the surface, but no quantitative characterization of the surface area and pore volume. The globule size, pore size distribution and mean pore diameters can be estimated, but the information provided is rough and limited.

Pore sizes and their distribution have been better characterized using other techniques. Through-pore size characterization has been done using mercury intrusion porosimetry (MIP) [13] and capillary flow porometry (CFP) [14]. Mercury intrusion porosimetry relies on bulk samples and provides information about blind and through-pores based on volume measurements. However, a key concern about MIP is the extent to which the porous properties of bulk and dry monoliths measured by MIP are really indicative of the chromatographic performance under capillary and wet conditions. Therefore, CFP which measures through pore size distribution in the capillary format using a gas as a displacing agent for a wetting liquid gives more accurate representation of the through-pore size distribution.

Mesopore size characterization has long been accomplished using nitrogen sorption isotherms (followed by BET calculations) [15] and inverse-size exclusion chromatography (ISEC) [16]. BET calculations utilize nitrogen adsorption and desorption curves for determining the mesopore size range and mesopore volume fraction, based on determination of surface area. It has been effectively used for silica monoliths and sometimes for organic monoliths as well [16]. However, measuring the mesopore volume by BET requires absolute drying of the sample, which would provide incorrect data if the polymeric skeleton shrinks on drying. Therefore, ISEC offers a better way of characterizing actual columns, and can provide the total porosity, external porosity and mesopore volume fraction. This is carried out using different molecular weight standards, such as polystyrene, and measuring their elution times. However, the use of polystyrene standards requires the use of organic solvents, such as tetrahydrofuran, as mobile phase, which may cause swelling of the polymeric monolith and, thereby, alter its porosity. Therefore, Li et al. [8] used different molecular weight proteins as standards, and determined the porosities of mildly hydrophilic polyethylene glycol diacrylate monoliths using aqueous solvents as mobile phases.

Despite this, ISEC is not used as often as MIP and BET for general purpose pore-size characterization, as it provides only limited information. Recently, Grimes et al. [17] formulated two models, the parallel pore model (PPM) and parallel network model (PNM) based on the first moment of column response to pulsed injections, to measure ISEC curves. They were able to calculate pore characteristics such as void fraction of mesopores and silica skeleton, pore volume distribution and connectivity of mesopores from these ISEC experiments.

Newer techniques, such as total pore blocking (TPB) [18] and confocal laser scanning electron microscopy (CLSM) [19] have also been used to determine pore characteristics of monolithic columns. Cabooter et al. [18] recently reported TPB for determining the external porosity of packed and monolithic columns. TPB is a pore filling process in which the inner pores are filled with hydrophobic solvent, and the retention time for a non-retained compound is measured. This retention time theoretically corresponds to the volume of the interstitial space, giving the external porosity of the column. CLSM gives the complete three-dimensional macropore morphology of a column [20], based on quantitative physical reconstruction of several microscopic images captured. This technique has not been applicable to polymeric monoliths because of difficulties involved in matching the refractive index of polymeric monoliths with silica tubing.

Overall, these techniques complement each other and aid in complete characterization of monolith morphology and porosity. However, one must be careful in choosing the technique, as it might alter the physical characteristics of interest during the measurement. A careful selection of characterization technique can provide great insight into parameters governing performance of particle packed as well as monolithic columns. Since, particle packed columns have been studied for many years and optimized with respect to bed structure, a short review of the factors governing their performance can provide important insights and comparison to monolithic bed structure. Therefore, the next section focuses on the bed structure of particle packed columns for both porous and core–shell particles.

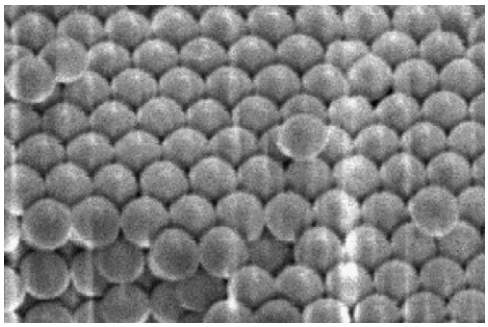

Fig. 1. SEM image of a capillary column packed with 1 μm particles.

3. Particle packed columns

The most common stationary phases used for liquid chromatography have been spherical particles. Columns packed with particles are available in a variety of lengths and diameters, starting with conventional (4.6 and 2 mm i.d.) to microbore (1 mm i.d.) and capillary (<0.5 mm i.d.) columns. The packed bed structure, governed by the size, shape, and orientation of the constituent particles, along with column geometry and size have been regarded as prime factors influencing chromatographic performance [21,22]. The bed structure of particulate columns has been characterized by a variety of statistical models and experimental techniques to provide information on external porosity, permeability, and uniformity. Recently, Tallarek et al. [23,24] reported the analysis of bed structure and its correlation with column performance for both particle packed and monolithic columns using the CLSM technique. The influence of stationary phase particle shape and column packing pressure on local radial distribution of flow rate and resultant column efficiency was studied by Lottes et al. [25] using X-ray computed tomography. These studies along with optimization of the column technology, particle morphology and operating parameters has greatly improved chromatographic performance, especially separation efficiency, of these particulate columns.

3.1. Particle packed column structure

A close packed arrangement, as shown in Fig. 1, should ideally be formed in columns packed with uniform size particles. A substantial improvement in separation performance with perfectly uniform packed columns was reported by Billen et al. [26] and Knox [27]. However, this ideal structure cannot be obtained in reality because of imperfections in the packing procedure. The structures of packed beds are typically found to be non-homogenous, both radially and axially [28]. Which has been attributed to packing instability, causing channeling in the packed bed structure, as well as the "wall effect" [27,29].

3.1.1. Effect of particle morphology on bed structure

The morphological features of the particles, such as size and shape, are known to influence bed uniformity and have been extensively studied to improve chromatographic performance. Reports have claimed more uniform bed structure with small particles as compared to large particles. The reason was ascribed by Lottes et al. [25] to be the extra packing force required to move larger particles to favorable positions, since they tend to block the paths of each other. However, the high back pressure associated with use of these small particles (sub-2 μm) limits further reduction in their size. In contrast, the uniformity of the column decreases with an increase in column permeability, since there is a proportional increase in defects in the packed bed [30]. Therefore, there is a tradeoff between chromatographic efficiency and column back pressure.

This compromise has led to discovery of alternate routes for improvement in column performance, such as the use of core–shell particles [31]. For such particles, the axial diffusion path within the stagnant mobile phase is greatly reduced since the material is only superficially porous. The decreased diffusion path should, in principle, decrease the C-term contribution to plate height in the van Deemter model [32]. This improved mass transfer also occurs in nonporous particles; however, increased efficiency occurs at the expense of sample loading capacity [5]. Thus, the porosity of the particle also contributes to column performance as it determines the bed structure at the microscopic scale.

In addition to small particle size, narrow particle size distribution (PSD) is also considered to be an important factor for improving column homogeneity and performance [33–35]. The narrow PSD associated with core–shell particles has been reported to be a major reason for their improved performance over conventional particle packed columns [31]. In contrast, others have reported column homogeneity to be better with broad PSD than with narrow size distribution [36,37]. The effect of PSD on plate height (H) and permeability was reported by Halasz and Naefe [38] to be negligible, until the PSD was less than 40% around the mean. Billen et al. [39] also supported this claim based on the relationship between particle size distribution and kinetic performance of packed columns. The presence of fines was reported to influence the column performance more than the PSD, since they filled the voids between the larger particles.

Particle shape has also been considered to be an important characteristic influencing packed column performance. Spherical particles have been reported by Lottes et al. [25] to give more homogenous bed structures than irregular ones. In contrast, De Smet et al. [40] reported better efficiency with diamond shaped pillars than with cylindrical or ellipsoidal ones for his pillar array columns. Moreover, the reduced plate height (H) was shown to be 2 times smaller for a perfectly ordered array of porous cylindrical pillars than for the best spherical particle packed columns via mathematical calculations [41]. However, there is one significant difference between particle packed and pillar array columns, i.e., the packing elements contact each other in particulate columns. Nevertheless, the influence of particle shape on column performance is clearly demonstrated by these studies. Surface roughness of the particle seems to be one more factor that influences column performance, as bed structure has been reported to be less dense with rough particles than with smooth particles [42].

3.1.2. Effect of column wall on bed structure

The column wall has been shown to be an important factor that contributes to column performance. The wall causes a radial variation of packing density, disturbing the particle packing close to the wall, termed the "wall effect" [43–45]. Two different wall effects have been reported by Shalliker et al. [46]. One is due to the rigid wall of the column which makes it impossible to pack the particles tightly against the wall. The second effect is due to friction between the bed and column wall, which makes it difficult to obtain a homogenous packing radially across the column. Recently, Tallarek et al. [23] confirmed and visualized these geometrical and friction-based wall effects in capillary columns by empirically analyzing the porosity profile of statistically derived packed beds.

Some authors have reported the thickness of the wall region to be a function of the column diameter [25], while others report it to be approximately several tens of particle diameters [47], irrespective of column dimensions. In capillary columns, heterogeneity near the wall has been found to be minimum with aspect ratios less than 10 (ratio of column to particle diameter), as the core region disappears and the packing structure is composed of only a wall region,

i.e., the packing structure becomes effectively more homogenous and ordered, thereby leading to excellent performance in terms of HETP. The reduced plate height was reported by Jorgenson et al. [2] to decrease with a decrease in column diameter. However, these changes in column efficiency could be attributed more to the change in particle diameter rather than column diameter, emphasizing packing density more than the wall effect [22,48].

Apart from particle and column dimensions, the column packing technique was found to contribute to bed density, causing differences in radial heterogeneity. In a dry-packed column, the permeability was reported to increase from the center to the wall, while for slurry packed columns, the permeability decreases from the center to the wall [27,49–51]. Farkas et al. [43] reported the presence of a homogenous core at the column center surrounded by a thick heterogeneous packing layer along the column wall, with no defined boundary in between. In contrast, Jorgenson et al. [52] reported the exact opposite, as they found particles to be more densely packed around the walls than in the center for capillary diameters greater than 75 μm.

3.2. Influence of bed structure on fluid flow through packed columns

There occurs a radial and axial variation in local mobile phase velocities as a consequence of the above stated radial and axial heterogeneities in the bed structures of chromatographic columns. Moreover, depending on the particle packing density near the walls, the velocity along the column wall may be slower or faster than in the core. Billen et al. [26] proved this via computational fluid dynamics simulations in a simplified two-dimensional mimic of particle packed columns, which was in agreement with results presented by Schure and Maier [30], indicating an increase in permeability with increased defects in the column packing. The latter study experimentally proved the mathematical predictions of Gzil and coworkers [53] regarding increased flow through the preferential flow path in the bed structure. The maximum velocity of the mobile phase in uniformly packed columns was found to be lower than that of non-uniformly packed columns. The solute traveled with a higher velocity through the preferential path, thereby traveling a greater distance than through the constricted bed area. Hence, the solute, introduced initially as a plug, became distributed in these different flow regions, which resulted in band broadening. Tallarek et al. [20] further verified this variation in porosity along the column length and related it to the transcolumn velocity gradients reported by Giddings. This study provided valuable insight into structure–transport relationships.

3.3. Performance of particle packed columns

The efficiency of chromatographic columns is expressed mathematically in terms of theoretical plates (N) or plate height (H), with lower plate height and higher theoretical plate count corresponding to better column performance. The performance of chromatographic columns is related to their bed structures. Therefore, the factors influencing bed structure also govern column performance. Assuming the use of spherical particles, the two major factors affecting the column efficiency are column and particle diameters.

3.3.1. Effect of column diameter

The efficiency of particle packed columns has been improved progressively over time with column miniaturization. Kennedy and Jorgenson [54] compared the efficiencies of packed capillary columns (28 and 50 μm i.d.) with conventional columns (9.4 mm i.d.). The 50 μm i.d. capillary column (30.1 cm long) gave 21,700 total theoretical plates (72,093 plates/m) compared to 8900 (35,600 plates/m) from a 25 cm long conventional column for bovine serum albumin (BSA). Although there was a difference in column length, it could not account for the difference in plate count. This improved performance for capillary columns has been attributed to reduced column heterogeneity with decrease in column diameter and, thereby, reduced A and C terms in the van Deemter equation [2].

Jorgensen et al. [2] observed the same with different capillary diameters (50–21 μm) packed with 5 μm porous octylsilane modified silica particles. The reduced plate height decreased from 1.4 to 1.0 (unretained analyte) with a corresponding decrease in column diameter. For a retained analyte, the value for the minimum h decreased from 2.4 to 1.5. This difference in h value resulted from greater longitudinal diffusion of the retained analytes. The column was operated under isocratic conditions with 10% acetonitrile and 90% sodium phosphate solution with 10^{-3} M EDTA (pH 7.0) as mobile phase.

In an another study, McGuffin and Novotny [3] reported a statistically significant reduction in plate height (0.160–0.120 mm) or increase in theoretical plate count (1.65×10^5 to 2.20×10^5, or 6250–8333 plates/m) for a decrease in column diameter from 100 to 60 μm (26.4 m columns). The results reported were obtained using toluene as analyte ($k = 0.01$) with 0.3% methanol in hexane as mobile phase.

3.3.2. Effect of particle diameter

In the same study, McGuffin and Novotny [3] showed the improved performance of capillary columns with decreasing particle size. An increase in the total plate count from 1.96×10^5 to 3.10×10^5 (7424–11,742 plates/m) with a decrease in particle size from 30 to 10 μm for a 26.4 m × 75 μm i.d. capillary column was reported. This difference in column performance was attributed to lower eddy diffusion in columns packed with smaller particles. Hirata and Jinno [55] proved the same by reporting 110,000 and 50,000 theoretical plates/m for 1 m × 0.2 mm i.d. glass columns packed with 3 and 10 μm, respectively. The columns were operated in the reversed phase mode for the separation of benzene derivatives, employing methanol as mobile phase. This improved performance with reduction in particle size was further supported in a study by Liu et al. [56]. A total plate count of 27,000 plates (180,000 plates/m) was reported for a 15 cm × 75 μm i.d. capillary column packed with 1.7 μm particles, in contrast to a plate count of 15,000 (100,000 plates/m) for 3 μm size particles in reversed phase chromatography.

Overall, the performance of packed capillary columns has been improved by packing more uniform bed structures, miniaturizing the column, optimizing the packing procedure and, most importantly, controlling the particle shape and morphology. Since there are some practical constraints, e.g., high back pressure associated with small particles and reduced column diameter, the use of core shell particles and monoliths have been proposed as alternative stationary phases to overcome these limitations.

4. Monolithic columns

Monoliths were first developed and successfully used for HPLC in the early 1990s with the work of Hjerten et al. [57] and Nakanishi and Saga [58]. They have been regarded as a substitute for particle packed columns, offering high permeability with good separation efficiency. Monoliths can be divided into two general categories: silica-based monolithic columns (prepared using sol–gel technology) and organic polymer based monoliths (prepared by chain polymerization reaction). Monoliths can be prepared by in situ polymerization of a pre-polymer solution and bonded chemically to the walls or cladded by tubing. This eliminates the need for

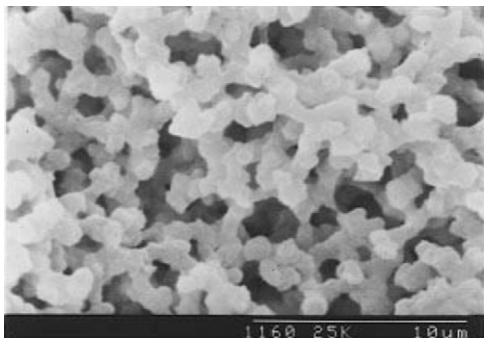

Fig. 2. SEM image of a silica monolith.
Reproduced with permission from Unger [59].

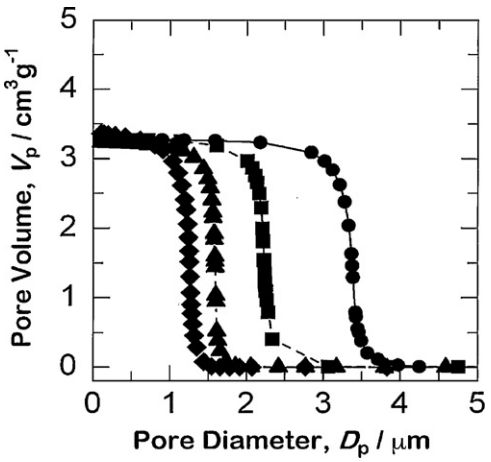

Fig. 3. Pore size distribution of heat-treated gels determined by mercury intrusion measurements. Each starting composition consisted of 0.01 M aqueous solution of acetic acid at 40 °C (100 mL) and TMOS (45 mL) with various amounts of PEO: ●, 9.4 g; ■, 9.8 g; ▲, 10.2 g; and ♦, 10.4 g.
Reproduced with permission from Nakanishi et al. [68].

retaining frits in capillary columns and also eliminates effort otherwise required for packing the column with particles.

As the performance of particle packed columns is determined by their bed structures, similarly the performance of monoliths (silica or organic) is governed by their morphology and pore structure which itself is affected by factors involved in their synthesis, such as nature of monomer and porogen along with polymerization conditions. The work of Tallarek et al. [20,24] using CLSM characterization has provided important insight in this regard. Therefore, monolith morphology (silica and polymeric) and the factors affecting their morphologies will be discussed in subsequent sections.

5. Silica monoliths

Silica monoliths have been successfully applied to the separation of both small and large molecules over the last 15 years [6]. Silica monoliths possess a spongy structure characterized by round pores [59] and a network skeletal structure as shown in Fig. 2 [60]. They have a surface chemistry similar to particle packed columns, but have been reported to have large through-pore/skeleton size ratio (1.2–2.5) as compared to 0.25–0.4 for particle packed columns [61,62]. As a consequence, they have 65% external porosity as compared to 25% for particle packed columns [63], thereby providing shorter diffusion path length in the stationary phase and lower flow resistance, simultaneously. These silica macroporous structures have also been reported to have a bimodal pore size distribution, with a significant fraction of mesopores. This section briefly explains the steps involved in preparation of silica monoliths followed by factors affecting their structure and, thereby, performance.

5.1. Preparation of silica monoliths

The preparation of silica monoliths consists of hydrolyzing a mixture of silane compounds in the presence of an inert compound, the porogen. There occurs spinodal decomposition (sol preparation and hydrolysis), giving rise to periodic domains (silica-rich and solvent-rich). These network structures are then frozen by gelation (washing and aging of the gel), yielding the final polymeric skeleton with through-pores and mesopores [64]. Unreacted monomer and porogens present after polymerization are removed from the column by washing with an appropriate solvent. Finally, the fabricated monolith may be modified with one or more reagents to provide the desired surface chemistry. Thermal initiation has been the most popular method for fabrication of these sol–gel monoliths in capillaries as well as in conventional column formats. However, recently Zare et al. [65] successful fabricated sol–gel monoliths using photo initiation in capillary columns and used them for capillary electrochromatography. Initially, silica monoliths shrank during polycondensation, leaving a wide gap along the column walls. Therefore, they were enclosed with thermally shrinkable peek tubing after synthesis. This problem was eliminated with reduction in the column diameter (i.e., fabrication in capillary columns) and with improvements in the polymerization recipe [66]. The structural domains (particulate or monolithic mass) can be tailored by modifying the composition of the starting polymerization mixture of monomer, porogen and catalyst; varying the time of polymerization; and changing the temperature.

5.2. Silica monolith structure

The skeletal structure of silica monoliths has been described as agglomerated silica particles with varying size and through-pore distributions governed by the above mentioned factors. The bed permeability is inversely related to the domain size, similar to that in particle packed columns; however, the overall permeability is higher for monolithic columns. Nakanishi and Soga [58] prepared their first monoliths by reacting solutions of TEOS and TMOS containing poly(sodium styrene sulfonate) (NaPSS) of different molecular weights. They reported interconnected morphology with well defined periodicity in the silica monolithic structure using NaPSS5 with a molecular weight of 10 kDa. The use of other molecular weight NaPSS gave gels with isolated domains or interconnected pores. Also, an increasing concentration of NaPSS at 40 °C caused a shift in morphology from isolated domains to interconnected pores. There have been many reports on the effect of various polymerization factors on the morphologies of silica monoliths [67]. The same authors used different porogenic reagents, such as HPAA (polyacrylic acid) and PEO (polyethylene oxide). The size distribution of the through pores was found to be considerably narrower with PEO, and varied in mean size with different PEO concentration as seen in Fig. 3 [68]. The range of porogen concentration resulting in a monolith was found to decrease with an increase in molecular weight of the porogen used. Apart from this, the average domain size (i.e., through-pore plus skeleton size) was found to be larger with an increase in time difference between phase separation and sol–gel decomposition [69].

The mesopore fraction in the silica monolith skeleton can be tailored by aging and drying (solvent exchange). The rates of formation of the pore network and the pore size distribution were found to vary with temperature [68]. The distribution was found to be broadened with an increase in temperature, but with a concomitant decrease in intrinsic porosity of the monolith. The same

study also showed that the pH of the wash liquid also influenced the mesopore size distribution, with a basic pH solvent having the maximum effect. Therefore, varying these parameters would alter the morphology of the monolith.

The composition of the pre-polymer solution and the temperature of polymerization govern the homogeneity of the monolith. Since most monolith synthesis reactions are exothermic, heat transfer must take place radially across the column and through the mold wall in which the monolith is made. Therefore, the center of the bed tends to be hotter than the region near the wall. Nakanishi and Soga [67] showed that the local porogen concentration governing the through-pore size distribution in the monolith is determined by the temperature of that region. Also, shrinking of the monolith after polymerization causes mechanical stress at the monolith-to-column wall boundary. This might result in a gap at the wall, creating a preferential flow path for the mobile phase. Therefore, these factors must be reduced for better chromatographic efficiency.

5.3. Performance of silica monoliths

Smaller domain size, high phase ratio (volume of mobile phase to stationary phase), and good bed homogeneity have long been emphasized for improving the separation efficiencies of monolithic structures [70]. Kobayashi et al. [71] found that monolithic and particle packed columns had similar minimum plate height values; however, the efficiencies of silica monolithic columns were found to decrease much less rapidly than packed columns with increasing mobile phase velocity. This was attributed to larger A coefficients and smaller C coefficients in the van Deemter equation for monolithic columns compared to particle packed columns. Recently, a kinetic plot analysis of silica monoliths and particle packed columns by Morisato et al. [72] revealed that monolithic columns with macropore diameter and skeleton thicknesses of 1 μm performed equivalent to a 3 μm particle column as shown in Fig. 4. In an another study by Minakuchi et al. [63], silica monoliths with smaller size skeletons resulted in van Deemter plots (for amylbenzene and insulin) with minimum plate heights at higher linear mobile phase velocities than for particle packed columns, as shown in Fig. 5. The slope of the curve was found to decrease with a decrease in the skeleton size. This was attributed to the short diffusion path length associated with the smaller skeleton size, which had less contribution to the plate height C term. The same authors studied the effect of domain size in the monolithic structure, and found that the plate height was reduced with a reduction in domain size [73]. Also, a smaller effect of mobile phase linear velocity on

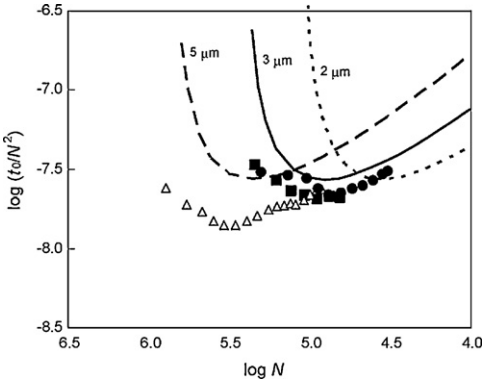

Fig. 4. Kinetic plots for reversed phase separation of amylbenzene with the monolithic silica columns and a Chromolith Performance RP-18e column, and calculated curves for the particle-packed column with particle diameter, d_p = 2, 3 and 5 μm. The curves were obtained using the following parameters: dynamic viscosity, η = 0.00046 Pa s, flow resistance, φ = 700, molecular diffusion coefficient in mobile phase, $D_m = 2.22 \times 10^{-9}$ m²/s, and Knox equation, $h = 0.65\upsilon^{1/3} + 2/\upsilon + 0.08\upsilon$, where h is reduced plate height ($h = H/d_p$), and υ is reduced velocity [11]. Filled circle: HPAAsilica column 1; filled square: HPAA-silica column 2; open triangle: Chromolith Performance RP-18e.

Reproduced with permission from Morisato et al. [72].

plate height for amylbenzenes was reported. The tendency was more pronounced for large molecules, such as insulin, since diffusion in the mesopores is slower for large molecules, which has a greater influence in the C term of the van Deemter equation.

In the same study, the authors estimated the optimum domain size for best performance, but found that the performance actually achieved was lower than that predicted [73]. The van Deemter plots indicated that the A coefficient increased and the C coefficient decreased with a decrease in domain size, suggesting that the mobile phase mass transfer was slower, although the small domain size facilitated faster mass transfer in the stationary phase [74]. Monoliths with small skeleton size were found to have greater irregularity in structure and wider through-pore size distribution, resulting in worse performance than expected [75]. Also, these silica monoliths were reported to have smaller phase ratio, resulting in poor resolution [76]. Desmet et al. [75] also showed theoretically that the performance of silica monoliths with small domain size can be greatly improved by increasing the homogeneity of the skeleton and through-pores, along with increasing the phase ratio. Hara et al. [70] synthesized silica monoliths with high phase ratio, small domain size and homogenous skeleton. They reported a plate height of 4.8 μm for a silica monolith with 2.2 μm domain size in a

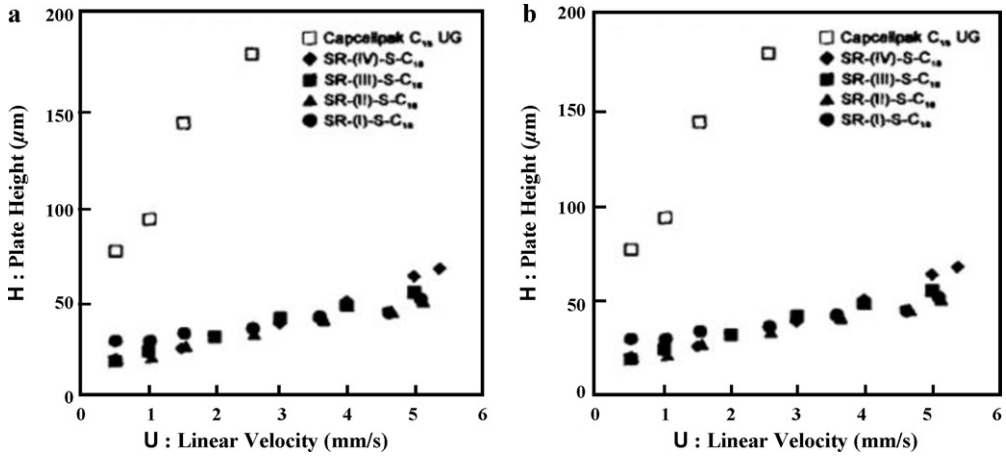

Fig. 5. Van Deemter plots for C_{18} silica rods and silica C_{18}-packed columns with 80% methanol as mobile phase. Solutes: (a) amylbenzene and (b) insulin.
Reproduced with permission from Minakuchi et al. [63].

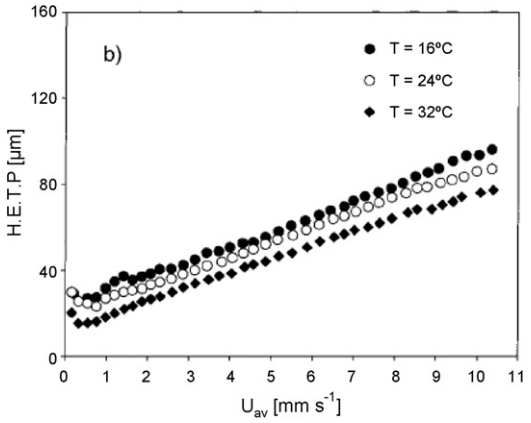

Fig. 6. Temperature dependence of the plate height curves for insulin on C18 silica monoliths with mesopore diameters of 20 nm.
Reproduced with permission from Leinweber et al. [77] (Copyright 2002 American Chemical Society).

15 cm × 100 μm i.d. column, which was better than that of a 3 μm particle packed column.

In addition to modification of the stationary phase bed structure, optimization of the chromatographic parameters can also improve column performance. Leinweber et al. [77] showed a decrease in plate height for insulin with an increase in temperature, as shown in Fig. 6, and assigned the reason to lower contribution of the A and C terms to the plate height in the van Deemter equation. This occurs because an increase in temperature increases both the lateral mass transfer and the intra-skeleton mass transfer.

Desmet et al. [78] showed that silica monolith performance could be better than particle packed column performance using kinetic plots. They also showed the existence of a desirable, but forbidden, region where no existing stationary phase support seems to operate, and indicated that synthetic methods are required to greatly improve the bed structure homogeneity and decrease the domain size for monoliths.

6. Organic monoliths

Organic monoliths were successfully developed and used for the first time in the 1990s when Hjertén et al. [57] prepared a highly swollen crosslinked gel of N,N-methylenebisacrylamide and acrylic acid in the presence of a salt in an aqueous medium. Since then, organic monoliths have been greatly improved, showing better performance for large molecule separations than silica monoliths because of their biocompatibility and large domain size morphology [79,80]. However, the performance of polymeric monoliths in the isocratic separation of low-molecular-weight organic compounds is relatively poor [9]. These differences in performance might be attributed to lack of mesopores or presence of micropores in the bed structures of the monoliths and structural inhomogeneity leading to flow dispersion [6,81]. Also, Nischang et al. [9] attributed this poor performance to heterogeneous gel porosity in the globular structure of the monolith, stemming from radial distribution of the crosslinker density in the globule. As a consequence, increased band dispersion for retained analytes slowly deteriorates the separation, and results in a totally unsuitable material for small molecule separation. There are many reviews in the literature that report organic monolith synthesis routes and performance, but with little emphasis on bed structure [79,82,83].

6.1. Preparation of organic monoliths

Capillary surface modification and initiation of polymerization in pre-polymer solution are two important steps involved in preparation of organic monoliths in capillary columns. First, the inner wall of the capillary is functionalized with a bi-functional reagent through a silanization reaction. Second, the capillary is filled with a pre-polymer mixture comprised of initiator, monomer(s) and porogen(s), and sealed at both ends with rubber plugs, followed by thermal or photo-initiated polymerization. During polymerization, monoliths are covalently bonded to the capillary surface, ensuring that the monolith can withstand relatively high pressures without being extruded from the capillary.

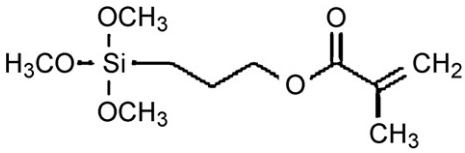

Fig. 7. Structure of TPM.

6.1.1. Modification of capillary surface

The capillary surface is usually modified with a bi-functional silanizing reagent such as vinyl silane, acrylate silane or methacrylate silane. The most common reagent used is 3-(trimethoxysilyl)propyl methacrylate (TPM) (Fig. 7) [84]. Generally, capillary surface modification involves capillary pretreatment, silanization and drying steps.

There have been many reports in the literature for optimizing the pretreatment and silanization procedures involved in surface modification. For example, Courtois et al. [84] compared 3 pretreatments and 11 silanization procedures by varying the parameters involved in them. The study showed that the etching step (using base) increased the roughness of the inner capillary surface along with silanol group concentration, both of which contributed to better adhesion of the monolith to the capillary wall. Vidic et al. [85] also showed pretreatment to be a critical step in surface modification, and found that 15% TPM in dry toluene solution worked best for silanization.

The above described two procedures involved either etching or leaching of the surface in the pretreatment step. However, Cifuentes et al. [86] proved that etching of columns with NaOH followed by leaching with HCl gave more reproducibile surface treatment. Therefore, the optimized capillary surface modification procedure included both etching and leaching steps.

6.1.2. Monolith synthesis

After surface treatment, the treated capillary is filled with a pre-polymer solution and exposed to UV light or heat. The monomers may consist of a functional monomer along with a crosslinker, or simply a single functionalized crosslinking monomer. Porogens can be low or high molecular weight inert chemicals responsible for generating pores in the monolith. There occurs differential phase separation in the homogenous precursor solution during polymerization, which is induced by porogenic solvents with different thermodynamic properties. The monomers and porogens, as well as the initiation method, greatly influence the polymerization mechanism and phase separation, thereby affecting monolith morphology, pore size distribution, and separation performance.

6.2. Organic monolith structure

Similar to particle packed columns and silica monoliths, the performance of organic monoliths is also determined by their bed structure morphology and porosity. Monoliths should have both large surface area and good permeability. A large surface area provides more active sites for effective interactions, and good permeability allows faster analysis and moderate back-pressure. Porosity is the most important morphology characteristic, as it

reflects the size and organization of both microglobules and clusters. Therefore, the morphologies of these monolithic structures, along with factors that influence the morphology, should be evaluated in order to optimize their performance.

6.2.1. Effect of initiation method

The initiation method and various parameters related to it such as temperature, light intensity, etc., govern the rate of polymerization reaction, which ultimately determines the monolith morphology. This section focuses on the initiation method, which may be radiation polymerization [87], living polymerization [88], high internal phase emulsion polymerization (HIPE) [89] and polycondensation [90]. Svec [81] recently published an excellent review describing the various approaches used for monolith synthesis. The different initiation methods give rise to different monolith morphology; for example, HIPE [89] gives an open pore monolith while thermal or photo initiation gives globular or fused morphology contingent upon other factors. Among these different initiation methods, thermal and photo initiation are more commonly used and will be discussed in detail.

6.2.1.1. Thermal initiation. Thermal initiation is one of the earliest methods used for organic monolith synthesis. For example, Svec and Frechet [91] successfully fabricated a porous poly(glycidyl methacrylate-co-ethylene dimethacrylate) monolith using 1% 2,2′-azobisisobutyronitrile (AIBN) as the thermal initiator. They also documented the effects of polymerization temperature, polymerization time, and type and concentration of thermal initiator on the morphology of the monoliths [92]. Viklund et al. [93] further showed that the pore size distribution of monoliths shifted toward smaller values with increased polymerization temperature and subsequent increase in surface area. They assigned the cause to higher decomposition rate of initiator and, subsequently, polymerization rate. An increase in temperature also resulted in an increase in solubility of the monomer, thereby resulting in late phase separation and large pore size; however, this effect had less influence than decomposition rate.

The polymerization time also changes the porosity of the fabricated monolith. As was observed by Svec et al. [94], the large pores disappeared upon prolonged polymerization, which were otherwise characteristic of the monolith in the early stages of polymerization. However, Trojer et al. [95] showed that the mesopore fraction increased significantly with a decrease in polymerization time, as BET measurements revealed a surface area increase from 26.8 m^2/g to 77.2 m^2/g on reduction of the polymerization time from 24 h to 45 min. This could be due to less crosslinking with shorter polymerization time. These results were also supported by Nischang et al. [9] who reported a decrease in column performance with increase in polymerization time. They attributed this to increased importance of resistance to mass transfer originating from stagnant mass transfer zones in the porous structures. However, polymerization time is not widely used to tailor the pore size distribution, since maximum rigidity requires sufficient polymerization time.

Initiator type and concentration also affect monolith morphology and porosity. A higher concentration of initiator was found to produce smaller microglobules as a consequence of a large number of free radicals [96]. The selection of a free radical initiator is governed, to some extent, by its decomposition temperature.

6.2.1.2. Photo initiation. Photo polymerization provides a number of advantages over thermal initiation. This initiation method significantly reduces the polymerization time from hours to minutes and also increases the range of solvents that can be used as porogens. Volatile organic solvents, such as ethyl ether, methanol and hexanes, can be used as porogens [97]. This broad range of porogen selectivity provides better control over the morphology and porosity of the monolith as compared to thermal initiation. Moreover, during thermal polymerization, there exists a thermal gradient along the radial direction of the capillary, as the polymerization reaction is exothermic and not all of the heat generated is dissipated uniformly throughout. Therefore, monoliths fabricated by photo initiation are more uniform compared to those made by thermal polymerization.

The factors governing photo polymerization are intensity and wavelength of the light source, as well as nature and concentration of the initiator. The former two remain constant with a particular lamp, while the latter two must be optimized for a good monolith. Some commonly used photo initiators are 2-methoxy-2-phenylacetophenone, 2,2-dimethoxy-2-phenylacetophenone and AIBN. Khimich et al. [98] studied the effect of initiator concentration and found that an increase from 0.2 to 1% led to an increase in polymer density and formation of uniform pore structure. In another study, Viklund et al. [99] found that a concentration of approximately 3–4% led to cracks in the continuous polymer structure. Although the type and concentration of initiator can be varied, they are not usually preferred. The influence of temperature on photo polymerization has been documented in the literature [100], but has been found to be less significant.

Although photo initiation has many significant advantages over thermal initiation, both are still equally used for monolith synthesis, and both affect the monolith morphology.

6.2.2. Effect of porogens

The porosity of the monolithic bed can be tailored by altering the natures of the porogenic solvents and/or their ratios without affecting the chemical composition of the final polymer. The porogens influence the pore properties of the monolith by controlling the solubility of the growing polymer chains in the polymerizing mixture and inducing differential phase separation in the homogenous precursor solution during polymerization [101]. Porogens can be classified as macro-porogens (those that create through pores) or meso-porogens (those that create mesopores), depending on the size of pores they create in the polymer skeleton. Generally, a poor solvent will generate larger through pores by facilitating early onset of phase separation. The new phase swells with the monomers because they are thermodynamically better solvents for the polymer than the porogen. As a consequence, large globules are formed with larger voids between them. In contrast, a good solvent generates smaller pores by delaying the onset of phase separation and competing for the monomer in solvating the nuclei.

The effect of porogen nature on porosity has been well documented in the literature. Viklund et al. [93] showed the effect of addition of a poor solvent on the pore size distribution in a poly(glycidyl methacrylate-co-ethylenedimethacrylate) monolith (GMA-EDMA). They reported an increase in the mode (pore diameter at the highest peak) of the pore size distribution curve from 150 nm to 2570 nm with an increase in percentage of dodecanol (poor solvent) from 0% to 15% as shown in Fig. 8a. On the other hand, addition of even a relatively small percentage of toluene (good solvent) resulted in a dramatic decrease in pore sizes for a poly(styrene-co-divinylbenzene) monolith (Fig. 8b).

The influence of porogen nature on monolith morphology and surface area was well documented in a study by Santora et al. [102]. In a non-polar divinylbenzene-styrene (DVB/STY) monomer system, the non-polar porogen, *n*-hexane, effectively generated high surface area, while the polar porogen, methanol, gave smaller surface area. They found that the solvent roles were reversed in a more polar ethylene dimethacrylate-methyl methacrylate (EDMA/MMA) monomer system, with hexane and methanol giving low and high surface area materials, respectively. SEM images (Fig. 9) showed

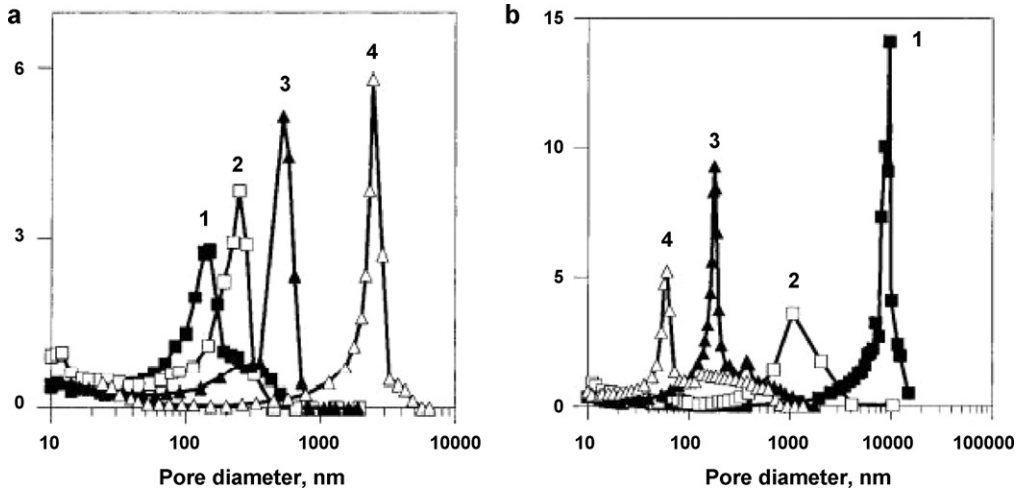

Fig. 8. Effect of dodecanol (a) and toluene (b) in the porogenic solvent on differential pore size distribution curves of molded poly(glycidyl methacrylate-*co*-ethylene dimethacrylate) and poly(styrene-*co*-divinylbenzene) monoliths. Conditions: 24 h polymerization time; (a) polymerization mixture: 70 °C, glycidyl methacrylate (24%), ethylene dimethacrylate (16%), cyclohexanol and dodecanol in mixtures 60 + 0 (1), 57 + 3 (2), 54 + 6 (3), and 45 + 15% (4); (b) polymerization mixture: 80 °C, styrene (20%), divinylbenzene (20%), dodecanol and toluene in mixtures: 60 + 0 (1), 50 + 10 (2), 45 + 15 (3), and 40 + 20% (4).
Reproduced with permission from Viklund et al. [93] (Copyright 1996 American Chemical Society).

that the monolith with high surface area had fused or very small micro-globule morphology as compared to monoliths with low surface area and large globular morphology. Although these polymers had surface areas as large as 820 m^2/g, it is unlikely that they would be permeable to flow since the pores were rather small. In another study, Premstaller et al. [103] found that a porogen mixture of decanol and tetrahydrofuran gave a poly(styrene/divinylbenzene) monolith with large through-pores and morphology similar to non-porous particles that have no micropores (termed micropellicular structure). These monolithic columns allowed rapid separation of oligo-nucleotides with high resolution.

Apart from the nature of the porogens, the ratio of porogens used can also influence the monolith morphology. Li et al. [104] successfully fabricated poly(bisphenol A dimethacrylate) (BADMA) monolithic columns with toluene and decanol as porogens, but found the porosity of these structures to be very sensitive to ratio of toluene and decanol. They also found that the monolith shrank and detached from the wall, which led to replacement of toluene with tetrahydrofuran (THF) as a good solvent. They also reported that monoliths with low back pressure had larger microglobules and microglobule clusters, while monoliths with high back pressure were composed of microglobules that were much smaller in size.

In addition to common organic solvents as porogens, solutions of a polymer in a solvent can also work as porogens. In a thorough study of the effects of poly(ethyleneglycol) (PEG) dissolved in 2-methoxyethanol on the pore properties of glycidyl methacrylate-co-trimethylolpropane trimethacrylate-co-triethylene glycol dimethacrylate) monoliths, Courtois et al. [105] found that the larger the molecular weight of the PEG, the larger the pores produced. Our group used PPG–PEG–PPG triblock copolymers and diethyl ether as porogens to prepare monolithic poly(ethylene glycol methyl ether acrylate-co-polyethylene glycol diacrylate) capillary columns [8]. These columns were found to have a considerable fraction of mesopores in the polymeric skeleton. In another study, a combination of high molecular mass polystyrene (PS) and chlorobenzene was used for the preparation of poly(glycerol dimethacrylate) (poly-GDMA) monoliths with an interesting morphology shown in Fig. 10 [106]. The structure of a poly-GDMA monolith prepared in situ with toluene as a poor

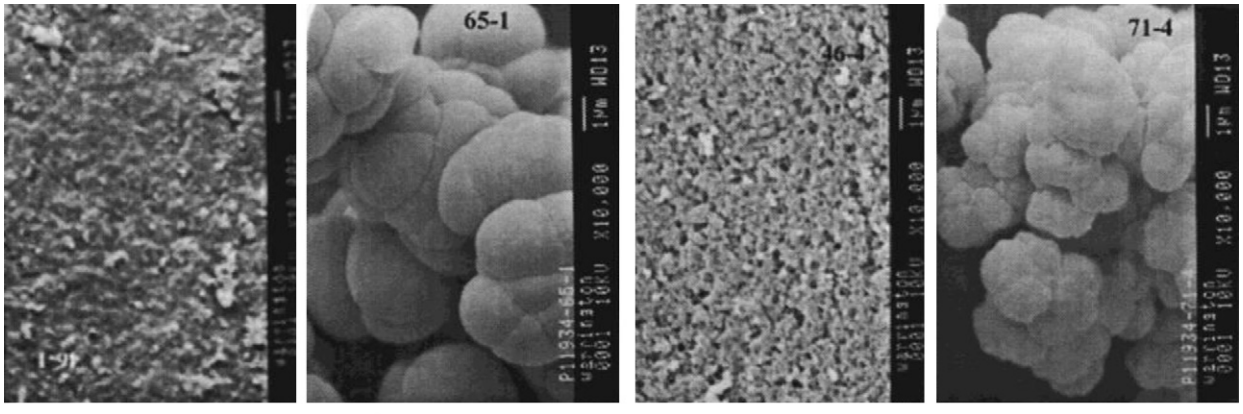

Fig. 9. SEM images of polymers at 10,000 magnification (1 μm bar in the upper right corner).
Reproduced with permission from Santora et al. [102] (Copyright 2001 American Chemical Society).

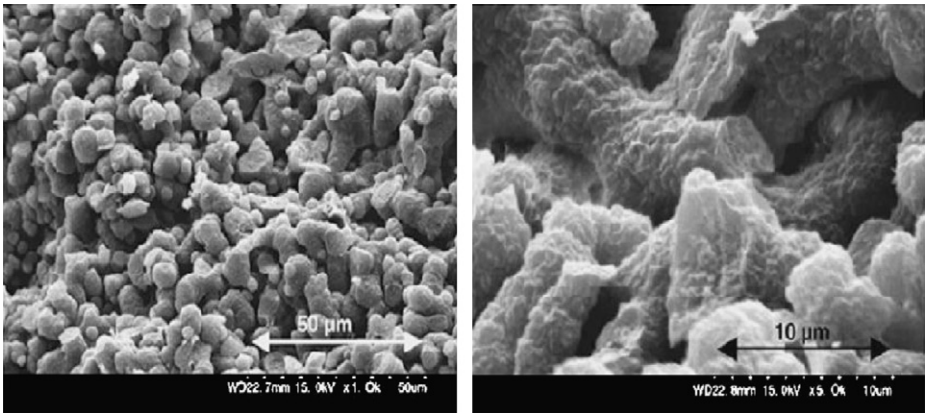

Fig. 10. SEM image showing the morphology of a poly(glycerol dimethacrylate) monolith prepared using a solution of polystyrene with a molecular mass of 3,840,000 in chlorobenzene.
Reproduced with permission from Aoki et al. [106].

porogenic solvent showed a typical agglomerated globular structure, whereas the morphology of a poly-GDMA monolith prepared in situ with the PS porogen was transformed from an aggregated globule form to a continuous skeletal structure. Along with this morphological transformation or change, the pore size distribution showed a sharp bimodal distribution, with one peak being located around 4 nm in the mesopore range (2–50 nm) and the other peak located around 1–2 μm in the macropore range (>50 nm), respectively.

Another atypical porogen used was supercritical carbon dioxide. Monoliths with a broad range of through-pore diameters (20 nm–8 μm) have been prepared using EDMA and TRIM as monomers [107,108]. The authors reported the direct dependence of properties such as pore size, pore volume, and surface area on CO_2 pressure. However, no applications of the resultant monolithic columns were reported.

Porogen selection still remains more of an art rather than a science and is primarily accomplished by experimentation. Researchers still prefer to look for appropriate porogenic solvents based on their experience and the published work of others. The above described monoliths demonstrated different performance for small and large molecule separations (discussed in Section 6.3.2).

6.2.3. *Effect of monomers*

A change in chemical properties of a monomer or amount of a monomer in the polymerization process not only changes the morphology and porosity of the bed structure, but it also changes the chemical composition of the monolith. The amount of crosslinker effects the globule size and morphology, as a higher concentration induces early phase separation, analogous to a poor solvent. Since crosslinking restricts the swelling of the globules, the pore size distribution shifts toward a smaller domain. A single monomer can also alter the polymerization kinetics and, thereby, the monolith morphology. It can also alter the surface chemistry and separation selectivity.

Smirnov et al. [109] showed a dramatic decrease in the size of the globules and, consequently, the size of the interstices between these globules (Fig. 11) with an increase in weight fraction of 2-hydroxyethyl methacrylate (HEMA) from 4% to 8% in the polymerization mixture. The authors attributed this to improved polymer–porogen interactions with an increase in the number of hydroxyl groups. Similar effects have also been shown for monomer mixtures such as GMA/EDMA and PS/DVB [93,110]. Santora et al. [102] also reported a decrease in surface area with a decrease in crosslinker ratio in the polymerization mixture. Xu et al. [111] investigated the effects of varying length and branching ratio of the crosslinker on column performance, keeping the molar ratio of the crosslinker and the monomer constant. They found that the volume of small mesopores increased with an increase in the length of the crosslinker, hence, leading to better separation efficiency for small molecules. These highly interconnected mesopores provided increased surface area and fast transfer kinetics for small alkylbenzenes. Thus, the effective thickness of the diffusion layer was significantly decreased.

The use of a single crosslinking monomer effectively increases the surface area and the concentration of desirable mesopores in the monolith, which has been demonstrated in several reports. Our group synthesized several monoliths from single crosslinking monomers, including bisphenol A dimethacrylate, bisphenol A ethoxylate diacrylate (BAEDA, EO/phenol = 2 or 4) and pentaerythritol diacrylate monostearate (PDAM) [104]. Among these monoliths, the morphology differed from one monomer to another. BAEDA-4 monoliths had a different morphology than BAEDA-2 monoliths. Distinct microglobules were not observed; instead, the monolith resembled a fused skeletal structure. Due to enhanced surface area resulting from highly crosslinked structure, separations of alkyl benzenes and alkyl parabens with high resolution were demonstrated using these columns.

Urban et al. [10] reported the use of a hypercrosslinking technique for extending the applicability of polymeric monoliths for small molecule separation. They used a mixture of styrene, vinylbenzyl chloride, and divinylbenzene monomers to prepare the monolith, followed by crosslinking of the functional groups on the surface using Friedal-Craft alkylation. The surface area of the monolith and the fraction of mesopores were significantly increased following hypercrosslinking.

6.2.4. *Effect of monomer to porogen ratio*

The effect of monomer concentration on the properties of the final polymer was recently demonstrated by Trojer et al. [95,112] for poly[p-methylstyrene-co-1,2-(p-vinylphenyl)ethane] monoliths. The macropore distribution shifted from 8.78 to 0.09 μm when the total monomer to porogen ratio was increased from 35% to 45% (v/v). The reason was attributed to a larger number of nuclei formed in the concentrated monomer system upon irradiation. As a consequence, these competing nuclei can touch each other before growing to larger size, resulting in small voids (through-pores) in the final monolith. Therefore, the monomer to porogen ratio should not be too high to prevent reasonable flow through the monolithic column. At the same time, the density and rigidity of the monolith should be observed, since they decrease with decrease in the initial

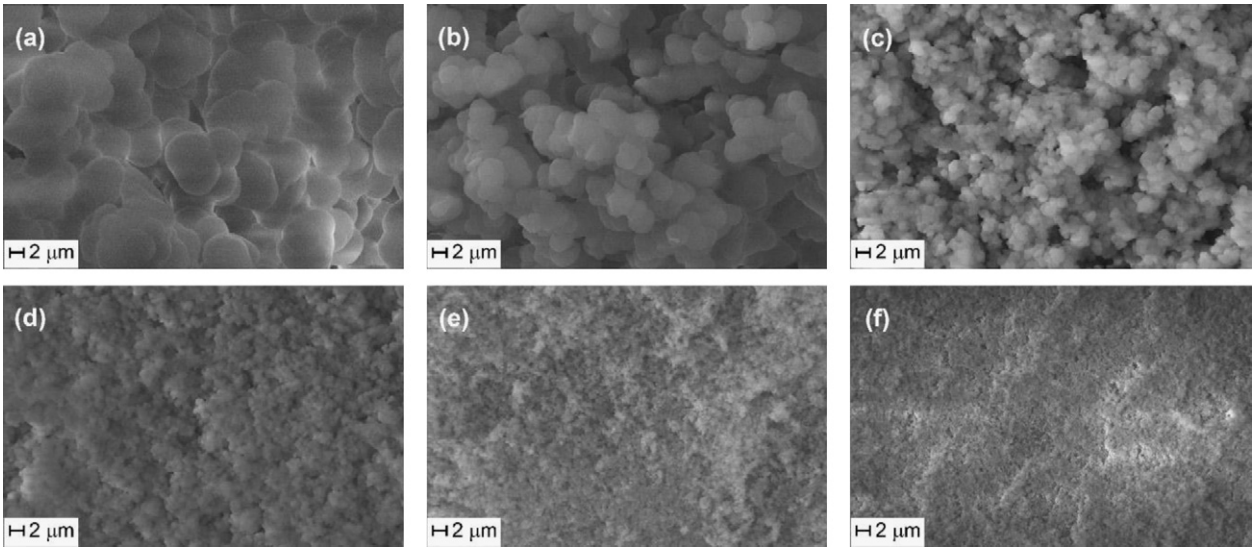

Fig. 11. SEM images of synthesized poly(DVB-co-EVB-co-HEMA) monoliths with different amounts of HEMA: (a) 10.5, (b) 11.9, (c) 13.2, (d) 14.7, (e) 17.9, and (f) 21.1%. Reproduced with permission from Smirnov et al. [109].

monomer concentration. A monomer concentration <0.5 g/mL for synthesis of a trimethylolpropane trimethacrylate (TRIM) monolith resulted in a powder [108]. The same was also observed for the synthesis of poly(triethylene glycol dimethacrylate) monoliths [113]. Monoliths prepared from a monomer concentration of 32.2 wt% could be stored dry, while those from 20.2 wt% could not be regenerated after drying. Smirnov et al. [109] showed a decrease in column permeability with an increase in monomer content in the polymerization mixture. Eeltink et al. [114] reported the preparation of low density methacrylate monoliths with broad porosity range when using a total monomer content of 20%.

6.3. Performance of organic monoliths

The major chromatographic performance characteristics (i.e., efficiency, resolution and permeability) of organic monolithic columns arise from the pore-size distribution and skeletal size, similar to that of any other stationary phase. Organic monoliths have been primarily used for large biomolecule separations (unlike silica monoliths, which have been used for both small and large molecules) and their morphologies have been reported to be globular in nature [115]. Recently, however, there have been reports of successful separations of small molecules using organic monoliths [9,113].

6.3.1. Effect of initiation method

The nature, time and condition of polymerization have been known to affect monolith morphology. The studies of Trojer et al. [95] and Nischang et al. [9] have shown lower polymerization time to be favorable for small molecule separation as a consequence of increased mesopore volume fraction. In thermal polymerization, the column performance has been reported to increase with an increase in polymerization temperature, as there occurs a decrease in though-pore size, thereby reducing the resistance to mass transfer and eddy term contributions in the van Deemter equation.

6.3.2. Effect of porogens

As described in Section 6.2.2, the porogens control the porosity of the monoliths, including pore-size and their distribution. Altering the type or the quantity of porogen determines whether the monolith can be used for small or large molecule separations and, also, the column performance for a particular separation. Premstaller et al. [103] demonstrated the performance of a monolithic column (with micropellicular morphology) for oligodexoynucleotide separations to be 40% better than particle packed columns. This was attributed to a reduction in intraparticle dispersion due to the complete absence of small pores in the monolithic skeleton, allowing only convective flow through the bed structure.

On the other hand, poly(BADMA) monolithic columns with small microglobules or fused morphologies were reported to be suitable for separation of small molecules such as alkylbenzenes and alkylparabens [104]. They gave efficiency measurements between 20,000 and 30,000 plates/m for uracil at 0.1 μL/min (i.e., 0.38 mm/s). The plate count was as high as 61,432 plates/m for retained compounds. The performance was attributed to small domain size and high surface area. In a study by Aoki et al. [106], the column efficiency was found to be 34,075 plates/m (H = 29.3 μm) when the monolith was prepared in situ with high molecular weight polystyrene as coporogen. This was much higher than 5650 plates/m (H = 177.0 μm), and 1335 plates/m (H = 749.3 μm) obtained from capillaries prepared in situ with low molecular weight standard PS or with toluene as porogens. These observations indicate that the high molecular weight PS porogenic solution delayed phase separation because of visco-elasticity. Li et al. [8,116] also reported size exclusion chromatography using organic monoliths prepared using poly(ethylene oxide)–poly(propylene oxide)–poly(ethylene oxide) (PEO–PPO–PEO) or PPO–PEO–PPO and Brij 58P as mesoporogens. The separations indicated the presence of mesopores in the skeletal structure.

6.3.3. Effect of monomers

In a study by Smirnov et al. [109], the column efficiency showed a significant increase (i.e., plate height decreased from 188 to 51 μm for an unretained compound) with an increase in HEMA content from 4% to 8% in the polymerization mixture. They attributed this to reduced globule size in the monolithic skeleton. Xu et al. [111] reported an increase in number of theoretical plates/m from 11,000 to 83,000 for thiourea with a change in crosslinker from ethylene dimethacrylate (EGDMA) to 2-methyl-1,8-octanediol dimethacrylate (2-Me-1,8-ODDMA). The increase was attributed to an increase in fraction of mesopores and, thus, reduced C term in the van Deemter equation. Urban et al. [10] reported an H value of 39 μm

Table 1
Representative performance data for a variety of packed and monolithic columns.

Stationary phase	Performance		k	Back pressure	Column dimensions	Reference
	N (plates/m)	H (μm)				
Particle packed columns						
Particle diameter						
5 μm	83,000	12.0	2.7	899 psi at 0.088 cm/s	33 cm × 50 μm i.d.	[2]
3 μm	110,000	9.1	0.9	Constant pressure of 200 kg/cm^2	100 cm × 200 μm i.d.	[55]
1.5 μm	209,000	2.4	0.2	23,000 psi at 0.145 cm/s	49.3 cm × 30 μm i.d.	[124]
1 μm	521,000	2.0	2.0	40,000 psi at 0.15 cm/s	46 cm × 30 μm i.d.	[122]
Silica monoliths						
Domain size						
3.1 μm	186,000	5.4	1.4	377 psi at 2.0 mm/s	14.5 cm × 100 μm i.d.	[70]
2.6 μm	200,000	5.0	1.4	537 psi at 2.0 mm/s	15 cm × 100 μm i.d.	[70]
2.2 μm	210,000	4.8	1.4	653 at psi 2.0 mm/s	15 cm × 100 μm i.d.	[70]
Organic monoliths						
Domain size						
N.A.	48,000	20.5	11.5 (estimated from chromatogram)	1740 psi at 6.4 mm/s	8 cm × 200 μm i.d.	[123]
N.A.	60,000	16.6	7.9	700 psi at 1.1 mm/s	16 cm × 75 μm i.d.	[104]
N.A.	83,200	12.0	0.04	3770 psi at 0.1 μl/min	13 cm × 100 μm i.d.	[10]

for benzene on their hypercrosslinked columns. They used the same column for rapid isocratic separation of peptides and gradient elution of 7 small molecules. They also demonstrated the use of this column for size exclusion of polystyrene standards using an organic mobile phase.

6.3.4. Effect of monomer to porogen ratio

Eeltink et al. [114] experienced an increase in separation efficiency for a small molecule by a factor of ~5, which they ascribed to broadening of the porosity curve when reducing the amount of monomers from 40 to 20%. In an another study, Trojer et al. [112] found the retention times for biomolecules to be unaffected by an increase in monomer content while the resolution increased. However, for small molecule separation (oligonucleotides), both the retention time and resolution were altered with change in monomer to porogen ratio, indicating a change in both mesopore volume and through-pore size. This also indicates that small molecule separations require broad pore distribution, as an increase in surface area increases small molecule interaction with the stationary phase.

Overall, the structures of polymeric monolithic columns determine their applicability. They have been effectively used for biomolecule separations with few applications for small molecules. Organic monoliths provided faster and more efficient separations than conventional HPLC columns (packed with 5 μm particles) for peptides in a kinetic plot study by Guillarme et al. [117], which they ascribed to improved mass transfer kinetics. However, with the advent of very small particle sizes the performance of organic monolithic columns lags behind that of particulate columns.

7. Conclusions

Monolithic column technology is still in its infancy, and discoveries in the field are expected to give rise to novel materials with unique properties. Monolith technology has been greatly improved over the past decade, and has been employed for both large and small molecule separations [118,119]. The performance of these monolithic columns has been shown to be comparable to particle packed columns (using the kinetic plot method) in some cases with silica monoliths [70]; however, it can still be significantly improved for polymeric monoliths, as is evident from Table 1. The kinetic plot study of Causon et al. [120] that compared the performance of organic monoliths to particle packed columns further verifies this. Silica monoliths have better rigidity and bimodal pore size distribution, whereas organic monoliths are more biocompatible and offer broad surface chemistry with which to work.

The published literature clearly indicates a dependence of column performance on stationary phase bed structure. Vervoort et al. [121] showed the effect of domain size (sum of the average sizes of the through-pores and skeleton) of monolithic columns on column efficiency by developing a structural model of the monolith. They calculated a minimum impedance value of 120 and reduced plate height of 0.8, a value equal to the reduced plate height of open tubular columns, and efficiency close to packed columns with no radial heterogeneity. The important conclusion in this study was that the domain size controls the efficiency of the column, and the random through-pore size distribution explains the limited performance of present monoliths. Therefore, by optimizing the bed structure and improving the homogeneity of the bed would significantly improve column performance.

Also, the applicability of globular organic polymer monoliths to large molecule separations and their poor performance for small molecules have been ascribed to the structure of the monoliths [9]. Therefore, future efforts should be directed toward better understanding of the relationship of monolith bed structure and performance, and control of through-pore structure and morphology. The stability and reproducibility of these monolithic stationary phases must also be improved to make them competitive with particle packed columns.

References

[1] M.S. Tswett, T.P. Varshav, Obshch. Estestvoistpyt., Otd. Biol. 14 (1903, publ. 1905) 20.
[2] R.T. Kennedy, J.W. Jorgenson, Anal. Chem. 61 (1989) 1128.
[3] V.L. McGuffin, M. Novotný, J. Chromatogr. 255 (1983) 381.
[4] J.H. Knox, M. Saleem, J. Chromatogr. Sci. 7 (1969) 614.
[5] P.W. Carr, D.R. Stoll, X. Wang, Anal. Chem. 83 (2011) 1890.
[6] G. Guiochon, J. Chromatogr. A 1168 (2007) 101.
[7] J.L. Liao, R. Zhang, S. Hjerten, J. Chromatogr. 586 (1991) 21.
[8] Y. Li, H.D. Tolley, M.L. Lee, Anal. Chem. 81 (2009) 4406.
[9] I. Nischang, O. Brüggemann, J. Chromatogr. A 1217 (2010) 5389.
[10] J. Urban, F. Svec, J.M.J. Fréchet, J. Chromatogr. A 1217 (2010) 8212.
[11] C. Liang, S. Dai, G. Guiochon, Anal. Chem. 75 (2003) 4904.
[12] J. Courtois, M. Szumski, F. Georgsson, K. Irgum, Anal. Chem. 79 (2006) 335.
[13] C. Salmas, G. Androutsopoulos, J. Colloid Interface Sci. 239 (2001) 178.
[14] Y. Fang, H.D. Tolley, M.L. Lee, J. Chromatogr. A 1217 (2010) 6405.
[15] J. Oxelbark, C. Legido-Quigley, C.S.A. Aureliano, M.-M. Titirici, E. Schillinger, B. Sellergren, J. Courtois, K. Irgum, L. Dambies, P.A.G. Cormack, D.C. Sherrington, E. De Lorenzi, J. Chromatogr. A 1160 (2007) 215.
[16] D. Lubda, W. Lindner, M. Quaglia, C.d.F.v. Hohenesche, K.K. Unger, J. Chromatogr. A 1083 (2005) 14.
[17] B.A. Grimes, R. Skudas, K.K. Unger, D. Lubda, J. Chromatogr. A 1144 (2007) 14.
[18] D. Cabooter, F. Lynen, P. Sandra, G. Desmet, J. Chromatogr. A 1157 (2007) 131.
[19] D. Hlushkou, S. Bruns, U. Tallarek, J. Chromatogr. A 1217 (2010) 3674.
[20] S. Bruns, U. Tallarek, J. Chromatogr. A 1218 (2011) 1849.
[21] S. Afandizadeh, E.A. Foumeny, Appl. Therm. Eng. 21 (2001) 669.
[22] I. Halasz, E. Heine, Nature 194 (1962) 971.

[23] S. Bruns, T. Hara, B.M. Smarsly, U. Tallarek, J. Chromatogr. A 1218 (2011) 5187.
[24] F.C. Leinweber, U. Tallarek, J. Chromatogr. A 1006 (2003) 207.
[25] F. Lottes, W. Arlt, M. Minceva, E.H. Stenby, J. Chromatogr. A 1216 (2009) 5687.
[26] J. Billen, P. Gzil, N. Vervoort, G.V. Baron, G. Desmet, J. Chromatogr. A 1073 (2005) 53.
[27] J.H. Knox, J. Chromatogr. A 960 (2002) 7.
[28] Q.S. Yuan, A. Rosenfeld, T.W. Root, D.J. Klingenberg, E.N. Lightfoot, J. Chromatogr. A 831 (1999) 149.
[29] B. Porsch, J. Chromatogr. A 658 (1994) 179.
[30] M.R. Schure, R.S. Maier, 30th International Symposium on High Performance Chromatography and Related Techniques, San Francisco, CA, June 17-22, 2006, paper L-0502.
[31] J.J. Kirkland, T.J. Langlois, J.J. Destefano, Am. Lab. 39 (2007) 18.
[32] N.N. Atia, P. York, B.J. Clark, J. Sep. Sci. 32 (2009) 2732.
[33] R.E. Majors, H.G. Barth, C.H. Lochmuller, Anal. Chem. 54 (1982) 323.
[34] R. Endele, I.n. Halasz, K. Unger, J. Chromatogr. 99 (1974) 377.
[35] C. Dewaele, M. Verzele, J. Chromatogr. 260 (1983) 13.
[36] R. Ohmacht, I. Halász, Chromatographia 14 (1981) 155.
[37] L.-I. Kulin, P. Flodin, T. Ellingsen, J. Ugelstad, J. Chromatogr. 514 (1990) 1.
[38] I. Halasz, M. Naefe, Anal. Chem. 44 (1972) 76.
[39] J. Billen, D. Guillarme, S. Rudaz, J.-L. Veuthey, H. Ritchie, B. Grady, G. Desmet, J. Chromatogr. A 1161 (2007) 224.
[40] J. De Smet, P. Gzil, N. Vervoort, H. Verelst, G.V. Baron, G. Desmet, J. Chromatogr. A 1073 (2005) 43.
[41] J. De Smet, P. Gzil, N. Vervoort, H. Verelst, G.V. Baron, G. Desmet, Anal. Chem. 76 (2004) 3716.
[42] M. Leva, M. Weinfraub, M. Grummer, M. Pollchik, H.H. Sforch, Fluid Flow Through Packed and Fluidized Systems, 1951.
[43] T. Farkas, G. Guiochon, Anal. Chem. 69 (1997) 4592.
[44] J.H. Knox, G.R. Laird, P.A. Raven, J. Chromatogr. 122 (1976) 129.
[45] J.E. Baur, R.M. Wightman, J. Chromatogr. 482 (1989) 65.
[46] R.A. Shalliker, B.S. Broyles, G. Guiochon, J. Chromatogr. A 888 (2000) 1.
[47] G. Guiochon, E. Drumm, D. Cherrak, J. Chromatogr. A 835 (1999) 41.
[48] S. Eeltink, G.P. Rozing, P.J. Schoenmakers, W.T. Kok, J. Chromatogr. A 1044 (2004) 311.
[49] M.L. Lee, Fundamentals of Analytical Separations, Brigham Young University, Provo, UT, 2010.
[50] C.H. Eon, J. Chromatogr. 149 (1978) 29.
[51] T. Frakas, M.J. Sepaniak, G. Guiochon, AIChE J. 43 (1997) 1464.
[52] K.D. Patel, A.D. Jerkovich, J.C. Link, J.W. Jorgenson, Anal. Chem. 76 (2004) 5777.
[53] P. Gzil, N. Vervoort, G.V. Baron, G. Desmet, J. Sep. Sci. 27 (2004) 887.
[54] R.T. Kennedy, W. Jorgensen, J. Microcolumn Sep. 2 (1990) 120.
[55] Y. Hirata, K. Jinno, J. High Resolut. Chromatogr. 6 (1983) 196.
[56] H. Liu, J.W. Finch, M.J. Lavallee, R.A. Collamati, C.C. Benevides, J.C. Gebler, J. Chromatogr. A 1147 (2007) 30.
[57] S. Hjerten, J.L. Liao, R. Zhang, J. Chromatogr. 473 (1989) 273.
[58] K. Nakanishi, N. Soga, J. Am. Ceram. Soc. 74 (1991) 2518.
[59] K.K. Unger, Porous Silica, Elsevier, Amsterdam, 1979 (Chapter 2).
[60] H. Minakuchi, K. Nakanishi, N. Soga, N. Ishizuka, N. Tanaka, Anal. Chem. 68 (1996) 3498.
[61] K.K. Unger, Porous Silica, Elsevier, Amsterdam, 1979 (Chapter 5).
[62] J.H. Knox, H.P. Scott, J. Chromatogr. 316 (1984) 311.
[63] H. Minakuchi, K. Nakanishi, N. Soga, N. Ishizuka, N. Tanaka, J. Chromatogr. A 762 (1997) 135.
[64] N. Tanaka, H. Kobayashi, N. Ishizuka, H. Minakuchi, K. Nakanishi, K. Hosoya, T. Ikegami, J. Chromatogr. A 965 (2002) 35.
[65] M. Kato, K. Sakai-Kato, T. Toyo'oka, M.T. Dulay, J.P. Quirino, B.D. Bennett, R.N. Zare, J. Chromatogr. A 961 (2002) 45.
[66] N. Ishizuka, H. Minakuchi, K. Nakanishi, N. Soga, K. Hosoya, N. Tanaka, J. High Resolut. Chromatogr. 21 (1998) 477.
[67] K. Nakanishi, N. Soga, J. Non-Cryst. Solids (1992) 14.
[68] K. Nakanishi, H. Minakuchi, N. Soga, N. Tanaka, J. Sol–Gel Sci. Technol. 13 (1998) 163.
[69] K. Nakanishi, J. Porous Mater. 4 (1997) 67.
[70] T. Hara, H. Kobayashi, T. Ikegami, K. Nakanishi, N. Tanaka, Anal. Chem. 78 (2006) 7632.
[71] H. Kobayashi, D. Tokuda, J. Ichimaru, T. Ikegami, K. Miyabe, N. Tanaka, J. Chromatogr. A 1109 (2006) 2.
[72] K. Morisato, S. Miyazaki, M. Ohira, M. Furuno, M. Nyudo, H. Terashima, K. Nakanishi, J. Chromatogr. A 1216 (2009) 7384.
[73] H. Minakuchi, K. Nakanishi, N. Soga, N. Ishizuka, N. Tanaka, J. Chromatogr. A 797 (1998) 121.
[74] N. Ishizuka, H. Kobayashi, H. Minakuchi, K. Nakanishi, K. Hirao, K. Hosoya, T. Ikegami, N. Tanaka, J. Chromatogr. A 960 (2002) 85.
[75] P. Gzil, N. Vervoort, G.V. Baron, G. Desmet, Anal. Chem. 76 (2004) 6707.
[76] N. Ishizuka, H. Minakuchi, K. Nakanishi, N. Soga, H. Nagayama, K. Hosoya, N. Tanaka, Anal. Chem. 72 (2000) 1275.
[77] F.C. Leinweber, D. Lubda, K. Cabrera, U. Tallarek, Anal. Chem. 74 (2002) 2470.
[78] P. Gzil, J. De Smet, G. Desmet, J. Sep. Sci. 29 (2006) 1675.
[79] E.G. Vlakh, T.B. Tennikova, J. Chromatogr. A 1216 (2009) 2637.
[80] N.W. Smith, Z. Jiang, J. Chromatogr. A 1184 (2008) 416.
[81] F. Svec, J. Chromatogr. A 1217 (2010) 902.
[82] F. Svec, J. Chromatogr. B 841 (2006) 52.
[83] F. Svec, A.A. Kurganov, J. Chromatogr. A 1184 (2008) 281.
[84] J. Courtois, M. Szumski, E. Bystrom, A. Iwasiewicz, A. Shchukarev, K. Irgum, J. Sep. Sci. 29 (2006) 325.
[85] J. Vidic, A. Podgornik, A. Strancar, J. Chromatogr. A 1065 (2005) 51.
[86] A. Cifuentes, P. Canalejas, A. Ortega, J.C. Diez-Masa, J. Chromatogr. A 823 (1998) 561.
[87] N.M. Vizioli, M.L. Rusell, M.L. Carbajal, C.N. Carducci, M. Grasselli, Electrophoresis 26 (2005) 2942.
[88] K. Kanamori, K. Nakanishi, T. Hanada, Adv. Mater. 18 (2006) 2407.
[89] C. Yao, L. Qi, G. Yang, F. Wang, J. Sep. Sci. 33 (2010) 475.
[90] C. Peskoller, R. Niessner, M. Seidel, J. Chromatogr. A 1216 (2009) 3794.
[91] F. Svec, J.M.J. Frechet, Anal. Chem. 64 (1992) 820.
[92] F. Svec, J.M.J. Frechet, Macromolecules 28 (1995) 7580.
[93] C. Viklund, F. Svec, J.M.J. Frechet, K. Irgum, Chem. Mater. 8 (1996) 744.
[94] F. Svec, J.M.J. Frechet, Chem. Mater. 7 (1995) 707.
[95] L. Trojer, C.P. Bisjak, W. Wieder, G.K. Bonn, J. Chromatogr. A 1216 (2009) 6303.
[96] S.H. Lubbad, M.R. Buchmeiser, J. Sep. Sci. 32 (2009) 2521.
[97] D.J. Throckmorton, T.J. Shepodd, A.K. Singh, Anal. Chem. 74 (2002) 784.
[98] G.N. Khimich, T.B. Tennikova, Russ. J. Appl. Chem. 78 (2005) 623.
[99] C. Viklund, E. Ponten, B. Glad, K. Irgum, P. Horstedt, F. Svec, Chem. Mater. 9 (1997) 463.
[100] M. Szumski, B. Buszewski, J. Sep. Sci. 32 (2009) 2574.
[101] E.C. Peters, F. Svec, J.M.J. Fréchet, C. Viklund, K. Irgum, Macromolecules 32 (1999) 6377.
[102] B.P. Santora, M.R. Gagne, K.G. Moloy, N.S. Radu, Macromolecules 34 (2001) 658.
[103] A. Premstaller, H. Oberacher, C.G. Huber, Anal. Chem. 72 (2000) 4386.
[104] Y. Li, H.D. Tolley, M.L. Lee, J. Chromatogr. A 1218 (2011) 1399.
[105] J. Courtois, E. Bystrom, K. Irgum, Polymer 47 (2006) 2603.
[106] H. Aoki, T. Kubo, T. Ikegami, N. Tanaka, K. Hosoya, D. Tokuda, N. Ishizuka, J. Chromatogr. A 1119 (2006) 66.
[107] A.I. Cooper, A.B. Holmes, Adv. Mater. 11 (1999) 1270.
[108] A.K. Hebb, K. Senoo, A.I. Cooper, Compos. Sci. Technol. 63 (2003) 2379.
[109] K.N. Smirnov, I.A. Dyatchkov, M.V. Telnov, A.V. Pirogov, O.A. Shpigun, J. Chromatogr. A 1218 (2011) 5010.
[110] T.B. Tennikova, B.G. Belenkii, F. Svec, J. Liq. Chromatogr. 13 (1990) 63.
[111] Z. Xu, L. Yang, Q. Wang, J. Chromatogr. A 1216 (2009) 3098.
[112] L. Trojer, S.H. Lubbad, C.P. Bisjak, G.K. Bonn, J. Chromatogr. A 1117 (2006) 56.
[113] Y. Li, H. Dennis Tolley, M.L. Lee, J. Chromatogr. A 1217 (2010) 4934.
[114] S. Eeltink, J.M. Herrero-Martinez, G.P. Rozing, P.J. Schoenmakers, W.T. Kok, Anal. Chem. 77 (2005) 7342.
[115] F. Svec, J. Sep. Sci. 27 (2004) 1419.
[116] Y. Li, H.D. Tolley, M.L. Lee, J. Chromatogr. A 1217 (2010) 8181.
[117] D. Guillarme, J. Ruta, S. Rudaz, J.-L. Veuthey, Anal. Bioanal. Chem. 397 (2010) 1069.
[118] R. Bakry, C.W. Huck, G.K. Bonn, J. Chromatogr. Sci. 47 (2009) 418.
[119] A. Canto-Mirapeix, J.M. Herrero-Martinez, C. Mongay-Fernandez, E.F. Simo-Alfonso, Electrophoresis 29 (2008) 4399.
[120] T.J. Causon, R.A. Shellie, E.F. Hilder, J. Chromatogr. A 1217 (2010) 3765.
[121] N. Vervoort, P. Gzil, G.V. Baron, G. Desmet, J. Chromatogr. A. 1030 (2004) 177.
[122] J.E. Macnair, K.D. Patel, J.W. Jorgenson, Anal. Chem. 71 (1999) 700.
[123] A. Greiderer, L. Trojer, C.W. Huck, G.K. Bonn, J. Chromatogr. A 1216 (2009) 7747.
[124] J.S. Mellors, J.W. Jorgenson, Anal. Chem. 76 (2004) 5441.